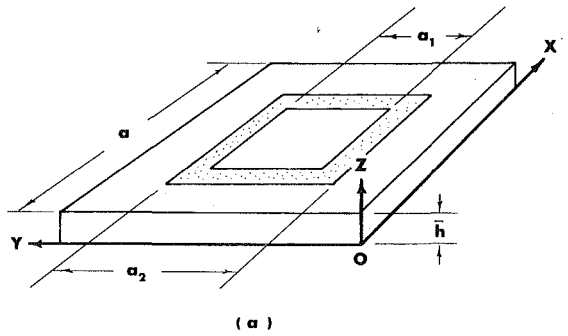

(a)

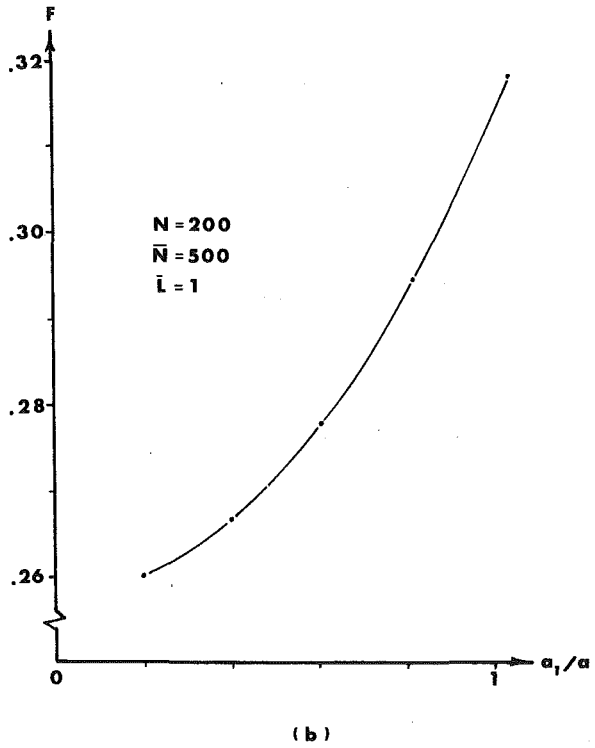

(b)

Fig. 5 Example 3: Nonuniform material properties: *(a)* pad geometry, *(b)* load capacity versus size of central region: $a = 1$, $\bar{h} = 0.1$, $h = 0.01$, $\bar{h} = -1$, $a_2 = a_1 + a/5$, $\rho = 1$, $\mu = 10^{-6}$, $\Phi_1^{zz} = 0.5 \times 10^{-6}$, $\Phi_2^{zz} = 0.75 \times 10^{-6}$, $\Phi_3^{zz} = 10^{-6}$, $\Phi_i^{xx} = \Phi_i^{yy} = \Phi_i^{zz}/2$

Since pressure is assumed to vary linearly throughout such an element, resultant statically equivalent concentrated nodal forces are given by

$$f_i = \frac{A}{12}\sum_{j=1}^{3}(1 + \delta_{ij})p_j \tag{A-5}$$

where

$$\delta_{ij} = 1, \quad i = j$$
$$= 0, \quad i \neq j \tag{A-6}$$

APPENDIX 2

Solid Elements for Porous Region

Suppose that density and viscosity are constant throughout a four-node tetrahedral element. Suppose further that local coordinate axes are principal axes of permeability and that principal values are constant throughout the element.[11]

It has been shown elsewhere [1, 10] that the fluidity matrix of such an element is given by

$$\bar{K}_{ij} = -\frac{\rho/\mu}{36V}(\Phi^{xx}b_ib_j + \Phi^{yy}c_ic_j + \Phi^{zz}d_id_j) \tag{A-7}$$

where

$$\begin{bmatrix} a_1 & b_1 & c_1 & d_1 \\ a_2 & b_2 & c_2 & d_2 \\ a_3 & b_3 & c_3 & d_3 \\ a_4 & b_4 & c_4 & d_4 \end{bmatrix} = \text{adj}\begin{bmatrix} 1 & 1 & 1 & 1 \\ x_1 & x_2 & x_3 & x_4 \\ y_1 & y_2 & y_3 & y_4 \\ z_1 & z_2 & z_3 & z_4 \end{bmatrix} \tag{A-8}$$

and

$$6V = \det\begin{bmatrix} 1 & 1 & 1 & 1 \\ x_1 & x_2 & x_3 & x_4 \\ y_1 & y_2 & y_3 & y_4 \\ z_1 & z_2 & z_3 & z_4 \end{bmatrix} = \sum_{1}^{4} a_k \tag{A-9}$$

[11] Very little loss of generality is incurred, since local coordinate axes can be varied element-by-element if desired.

DISCUSSION

S. M. Rohde[12]

The authors have presented an interesting application of the finite element method (FEM) to the incompressible porous bearing problem. Certainly one can envisage applications of the type presented in this paper where advantage can be taken of the ability of the finite element method to model complex geometries conveniently. This is particularly true in the porous solid.

We have recently applied finite element methods to compressible porous bearing problems in which the flow in the porous medium was assumed to be unidirectional. Excellent results were obtained using relatively few higher order (cubic) elements. Have the authors experimented along these lines?

Letting $\bar{L} = 1$ essentially, I believe, corresponds to the assumption a unidirectional flow in the porous medium (since linear elements are being used), which is probably a reasonable assumption for the case considered. This, along with the severely distorted solid elements, (as discussed by the authors) would probably explain the loss of accuracy with $\bar{L} = 2$. On the other hand, the fact that the nodal flows sum "exactly" to the net squeeze rate is somewhat to be expected if one chooses the appropriate nodal areas—as these are the finite element equations!

Let us now turn to an aspect of the FEM which is often taken for granted—the triangulation. To illustrate the effect of triangulation consider the case of an incompressible squeeze film between parallel impermeable square plates. The pressure distribution satisfies

$$\nabla^2 p = -1 \tag{19}$$

in the square and vanishes on the boundary of the square. As is well known, if one uses a rectangular triangulation and linear elements as the authors have done, the discrete finite element operator corresponding to the left-hand side of (19) is the usual five point difference "star," L_{ij} where

[12] Research Laboratories, General Motors Corp., Warren, Mich.

TABLE 1

Mesh spacing h	Case #1 FDM or uniformally sloping FEM (Fig. 6A) W*	P_{center}	Case #2 FEM (Fig. 6B) W	P_{center}	Case #3 FEM (Fig. 6C) W	P_{center}	Case #4 FEM (Fig. 6D) W	P_{center}
1/4	0.02881	0.07031	0.02734	0.06250	0.02832	0.06771	0.02930	0.07292
1/6	0.03216	0.07212	0.03149	0.06802	0.03204	0.07087	0.03227	0.07336
1/10	0.03403	0.07310	0.03379	0.07135	0.03401	0.07267	0.03405	0.07352
1/20	0.03486	0.07353	0.03480	0.07300	0.03486	0.07342	0.03486	0.07363
1/40	0.03507	0.07364	0.03506	0.07348	0.03507	0.07361	0.03507	0.07366
Exact	0.03514	0.07367						

* W is defined as: $W = h^2 \Sigma P_{ij}$.

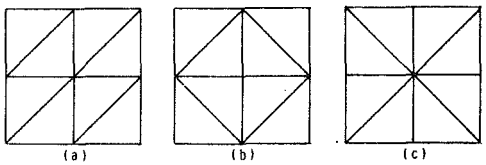

Fig. 6

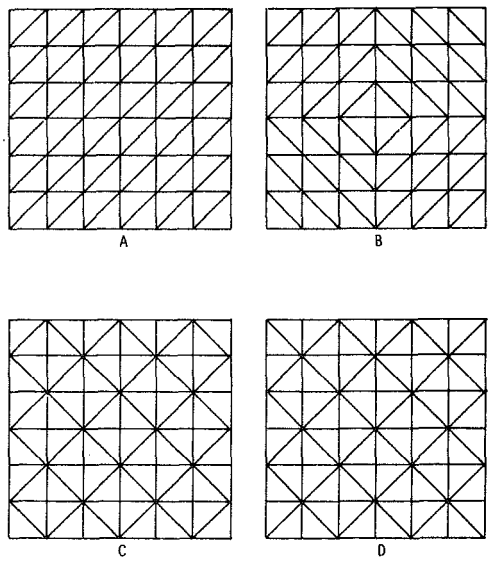

Fig. 7

$$L_{ij}(P) = P_{ij+1} + P_{ij-1} + P_{i+1j} + P_{i-1j} - 4P_{ij}. \quad (20)$$

On the other hand, the discrete form of the right-hand side of equation (19) *depends on the triangulation.* In Fig. 6 we see three types of points which may arise. The FEM equation corresponding to these three types of points are

$$L_{ij}(P) = -h^2 \quad (21a)$$

$$L_{ij}(P) = -\frac{2}{3}h^2 \quad (21b)$$

$$L_{ij}(p) = -\frac{4}{3}h^2 \quad (21c)$$

respectively, where h is the mesh spacing (which, without loss of generality is assumed to be uniform). A given triangulation may contain A, B, and C "type" points. To be more specific if the hypotenuses of all triangles slope the same way (Fig. 7A), all points are of type A, and we recover the usual finite difference solution. On the other hand, if one uses a mesh such as shown in Fig. 7B, one sees that the center is a type B point whereas the remaining points are type A. Clearly the solution obtained with this triangulation lies everywhere below that corresponding to the triangulation (2A). The triangulation used by the authors consists of alternate type B and C points according to whether $i + j$ is even or odd, respectively, as shown in Fig. 7C. Altering the parity, i.e., interchanging type B and C points, we obtain the triangulation shown in Fig. 7D.

Table 1 shows numerical results for the four triangulations compared with the exact solution. The latter was obtained from a series solution as discussed in [13].[13] One sees that the triangulations rank as #4, #1, #3, #2 in order of "accuracy"—although the differences between these become insignificant as $h \to 0$. Conversely for a given accuracy/computation one sees that some attention should be given to the choice of a triangulation. In fact the present comparison was motivated by the application of FEM to a dynamically loaded bearing—a situation in which one clearly seeks to minimize the degree freedom vector!

Finally, perhaps it is appropriate at this point to mention the fact that the Reynolds boundary condition can be incorporated with finite elements. Implementation is particularly easy with linear or certain quadratic elements using a point iterative method (e.g., Christopherson). For a detailed discussion see [14].

References

13 Hays, D. F., "Squeeze Films for Rectangular Plates," ASME Paper No. 62-Lub S-9, 1962.

14 Rohde, Steve M., and McAllister, G. T., "A Variational Formulation for a Class of Free Boundary Problems Arising in Hydrodynamic Lubrication," *Int. J. Engrg Sci.*, Vol. 13, 1975, pp. 841–850.

Authors Closure

Dr. Rohde makes a number of very helpful observations concerning application of the FEM to lubrication with *and* without surface porosity. Though our own experience in such studies has been largely limited to lower-order (linear) elements, his reported success with higher-order (cubic) elements is most encouraging[14]. However, one might be concerned by the conceptual loss occasioned by use of "non-physical" degrees of freedom, as well as by any consequent imposition of constraints on inter-element continuity of physical and geometrical properties. For these and other reasons (including sheer simplicity), we believe lower-order elements will probably dominate applied analysis of lubrication even more than they have that of structural mechanics.

(Closure continued on p. 186)

[13] Numbers 13–14 in brackets designate Additional References at end of discussion.

[14] Reference [7] of present reference [5] reports the experience of others with higher-order elements.

(Closure continued from p. 180)

The rigorous and detailed study of the effects of different triangularization schemes is fascinating, though of course such effects are fairly unpredictable with irregular geometries and (presumably) unimportant with sufficiently fine meshes. They should be both predictable and important in a large class of applications, however, and further study of mesh choice is thus clearly indicated.

We appreciate the additional suggested explanation for the paradoxical loss of accuracy shown in Fig. 3(b) with increasing $\bar{L}$ (and $\bar{N}$) for fixed $N < 120$. Incidentally, such convergence studies as Fig. 3 can be condensed and clarified by plotting error against $1/N$ instead of N, as was suggested by Dr. Pan in oral discussion. Further, the rational use of non-dimensionalization, deliberately avoided in the present expository paper, could be helpful as well.

All of the accuracy questions noted above can be resolved (in principle at least) through use of a sufficiently large number of simple linear elements, both plane and solid. In practice, however, the number of nodal degrees of freedom (largely used in describing the porous solid) may become uneconomic before such a happy state can be reached. If calculation of flow details within the porous solid is not required, order of the final problem can be reduced substantially by a simple device:

Assuming homogeneous boundary conditions, relation (13) for the porous solid region can be numerically reduced (condensed) to give

$$\{\bar{q}_1\} = [\bar{K}_{11}^*]\{\bar{p}_1\} - \{\bar{q}_1'\} \tag{13'}$$

Combining relations (12), (13'), (15), and (16) then gives the system relation

$$\{\bar{q}_1 + q\} = [\bar{K}_{11}^* + K]\{\bar{p}_1 = p\} + [S]\{\dot{h}\} \tag{17'}$$

which is of the *form* of relation (17) but of considerably lower *order,* since only nodes in the film region are involved.

The condensation procedure suggested offers no real economies if only one solution is required. In many practical cases, however, the same porous region is matched to a series of successively altered film regions, and in such cases the potential savings are substantial.

As Dr. Rohde suggests, the fact that numerical values of *system* nodal flows sum "exactly" to the next squeeze rate is indeed a direct consequence of the "built-in" satisfaction of continuity on an *element* basis. Similarly, columns (and rows) of pressure fluidity matrices $[K]$ must sum to zero. (The situation in structural mechanics is entirely analogous with respect to the equilibrium of nodal forces and the properties of stiffness matrices.)

Implementation of film rupture models in FEM analysis is a timely topic, and the suggested reference [14] an important one. Other approaches are now beginning to appear in theses and reports as well.

We hope that the excellent oral and written discussion prompted by this paper is evidence of growing interest in and utilization of the FEM in lubrication. In particular, we hope others will soon report the convincing examples of complex geometries contemplated by Figure 1 but, unfortunately, not carried out in the present paper.

Finally, and quite incidentally, readers generally interested in the application of FEM to lubrication should note the Errata to reference [5] which appears on p. 39 of this issue.